

pubs.acs.org/Macromolecules Article

Scaling of Polymer Solutions as a Quantitative Tool

Andrey V. Dobrynin,* Michael Jacobs, and Ryan Sayko



Cite This: Macromolecules 2021, 54, 2288-2295

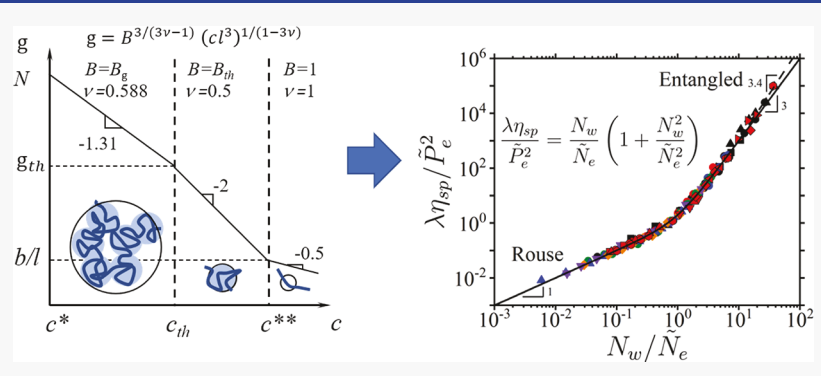


ACCESS

Metrics & More



SI Supporting Information



ABSTRACT: Knowledge of interaction parameters and Kuhn length for a polymer/solvent pair is a foundation of polymer physics of synthetic and biological macromolecules. Here, we demonstrate how to obtain these parameters from the concentration dependence of solution viscosity. The centerpiece of this approach is the scaling relationship between solution correlation length (blob size) $\xi = lg^{\nu}/B$ and the number of monomers per correlation blob g for polymers with monomer projection length l. The values of parameter B and exponent ν are determined by solvent quality for the polymer backbone, chain Kuhn length, and types and strength of monomer—monomer and monomer—solvent interactions. Parameter B assumes values B_g , B_{th} , and 1 for exponent $\nu = 0.588$, 0.5, and 1, respectively. In particular, we take advantage of the linear relationship between specific viscosity η_{sp} in the unentangled (Rouse) regime and the number of correlation blobs N_w/g per chain with the weight average degree of polymerization, N_w , and $g = B^{3/(3\nu-1)}(cl^3)^{1/(1-3\nu)}$ as a function of monomer concentration, c, and the corresponding B parameter. The values of the B parameters are extracted from the plateaus of normalized specific viscosity $\eta_{sp}(c)/N_w(cl^3)^{1/(3\nu-1)}$ or their locations as a function of the monomer concentration c in different solution regimes. The extension of the approach to entangled polymer solutions provides a means to obtain the chain packing number, P_{cr} and to complete the set of parameters $\{B_g, B_{th}, P_e\}$ (a system "fingerprint") uniquely describing static and dynamic solution properties of a polymer/solvent pair. This approach is illustrated for solutions of poly(ethylene oxide) in water, poly(styrene) in tetrahydrofuran and toluene, poly(methyl methacrylate) in ionic liquids, and sodium carboxymethylcellulose in water at high salt concentrations.

INTRODUCTION

The scaling approach has transformed our understanding of polymers by highlighting a universality in system properties and by classifying them in terms of characteristic power laws of monomer concentration and chain degree of polymerization. 1-13 This approach relies on the existence of a characteristic microscopic length scale defining macroscopic system properties. In polymer solutions, it is the solution correlation length (correlation blob size); 1-3,12,14 for chains and networks undergoing deformation, it is the size of a tension blob, 15-19 while in the case of polymer brushes, it is the distance between chain grafting points. 20-24 The common feature among all these systems is that on length scales smaller than the characteristic length scale, chain conformations remain unperturbed by the surrounding environment or by applied external forces. Furthermore, scaling allows a universal data representation independent of polymer-specific properties such as Kuhn length and monomer-monomer and monomersolvent affinity that are implicitly taken into account by a scaling exponent ν relating the characteristic length scale ξ with the number of monomers in it, $\xi \sim g^{\nu}.^{1,12,14}$

In polymer solutions, one can be even more quantitative by representing data in terms of the ratio c/c^* , of monomer concentration c to the chain overlap concentration c^* , by hiding system-specific properties in the c^* definition. ^{1,12,14} Unfortunately, this representation breaks down at monomer concentrations where chain conformations on length scales of the solution correlation length change from those at overlap concentration and specific features of the polymer/solvent pair

Received: December 20, 2020 Revised: January 27, 2021 Published: February 12, 2021





(Kuhn length and interaction parameters) become important. At these concentrations, the scaling approach settles on qualitative power law analysis of different solution regimes. Here, we show how to overcome these shortcomings and transform the scaling approach into a quantitative tool by obtaining chain Kuhn length and polymer/solvent-specific parameters, which we call B parameters, from analysis of the viscosity data. In particular, knowledge of these parameters allows us to calculate solution correlation length and use it to represent solution viscosity in a universal form by expressing it in terms of the number of correlation blobs per chain. Extending this approach to entangled polymer solutions, we obtain the chain packing number P_e and complete the set $\{B_{g}, P_e\}$ B_{th} , P_{e} of system-specific parameters. This set provides a means to quantitatively describe static and dynamic solution properties of a polymer/solvent pair in different concentration regimes. We begin with a brief overview of the scaling model of semidilute polymer solutions.

■ THE SCALING MODEL

The scaling model of polymer solutions relies on the existence of a characteristic length scale—solution correlation length ξ —defining a length beyond which all interactions are screened. This results in a chain with a degree of polymerization N (the number of chemical monomers per chain) on length scales larger than the solution correlation length (blob size) ξ each containing g chemical monomers to behave as an ideal chain of N/g blobs with size (square root of the mean-square end-to-end distance)

$$R = \xi (N/g)^{0.5} \tag{1}$$

The degree of polymerization N in a monodisperse system of chains with molar mass M and made of monomers with molar mass M_0 is equal to $N = M/M_0$. Throughout the paper, we express all parameters in terms of chemical monomers.

Inside the correlation blobs, chain statistics is determined by polymer—polymer and polymer—solvent interactions, which are manifested in the hierarchical blob structure shown in Figure 1a. In polymer solutions under good solvent conditions, correlation blobs are made of thermal blobs with size D_{th} and having g_{th} monomers each. On length scales smaller than the

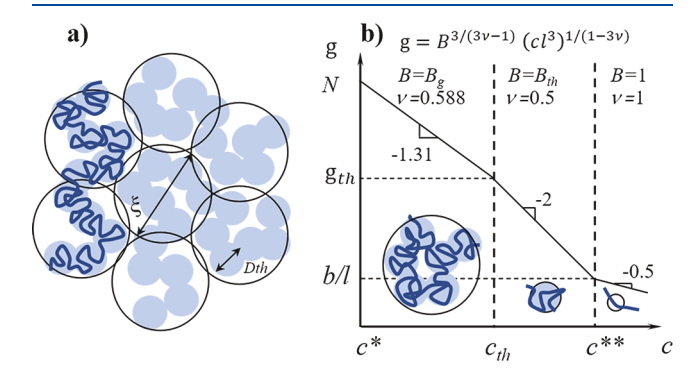


Figure 1. (a) Schematic representation of hierarchy of length scales in semidilute polymer solutions in a good solvent. Correlation blobs with size ξ contain thermal blobs with size D_{th} . (b) Concentration dependence of the number of monomers g per correlation blob. c^* - chain overlap concentration, c_{th} - thermal blob overlap concentration, and c^{**} - crossover concentration to the concentrated solution regime. Insets show the chain structure on the length scales of correlation blobs. Logarithmic scales.

thermal blob size, $r < D_{th}$, polymer—polymer interactions are weak, and the conformation of a section of a chain consisting of g_r monomers is that of an ideal chain with monomer projection length l, which for a carbon backbone is equal to 0.255 nm, and Kuhn length b

$$r = \sqrt{lbg_r} = lg_r^{0.5}/B_{th}, \text{ for } b < r \le D_{th}$$
(2)

The parameter $B_{th} = (l/b)^{0.5} < 1$ characterizes chain bending rigidity and is inversely proportional to the square root of the number of monomers per Kuhn length, b/l. Thus, knowing the value of the B_{th} parameter, we can calculate chain Kuhn length, $b = lB_{th}^{-2}$, in the solution.

On length scales $D_{th} < r \le \xi$, polymer—polymer interactions are dominant, and chain statistics is that of a self-avoiding walk of thermal blobs

$$r = D_{th}(g_r/g_{th})^{\nu} = lg_r^{\nu}/B_g, \text{ for } D_{th} < r \le \xi$$
 (3)

where v = 0.588 is the self-avoiding walk exponent. Taking into account eq 2, we can express the parameter $B_{\rm g}$ in terms of the number of monomers per thermal blob and chain Kuhn length as follows

$$B_{g} = lg_{th}^{0.588}/D_{th} = (lg_{th}^{0.176}/b)^{0.5}$$
(4)

Thus, depending on the number of monomers per thermal blob g_{th} , determining solvent quality for the polymer backbone and the number of monomers per Kuhn length b/l, $B_{\rm g}$ could be larger or smaller than unity.

By changing monomer concentration, one changes the number of blobs per chain and their structure on the length scale of the solution correlation length, ξ . To account for this, a scaling relationship between ξ and g is written in the following general form

$$\xi = \lg^{\nu}/B \tag{5}$$

where the exponent v = 0.588 or 0.5, and the *B* parameter is equal to B_g or B_{th} depending on the solution concentration regime as discussed below.

Concentration dependence of the correlation blob ξ and the number of monomers in it g follows from the space filling condition—the monomer concentration inside the blobs is equal to the solution monomer concentration, $c = g/\xi^3$. This expresses solution correlation length

$$\xi = lB^{1/(3\nu-1)}(cl^3)^{\nu/(1-3\nu)} \tag{6}$$

and the number of monomers per correlation volume

$$g = B^{3/(3\nu - 1)} (cl^3)^{1/(1 - 3\nu)}$$
(7)

as functions of monomer concentration, c, and the corresponding B parameter.

The chain overlap concentration (crossover concentration to the semidilute solution regime) is obtained by extrapolating the number of monomers per correlation length to the chain degree of polymerization, g = N,

$$c*l^3 = B_g^3 N^{(1-3\nu)} (8)$$

Thus, eq 8 correlates the interaction parameter B_g with the chain overlap concentration c^* , the degree of polymerization N, and monomer projection length l.

In semidilute polymer solutions $c>c^*$, crossover concentrations between different solution concentration regimes are determined by comparing correlation blob size ξ

with thermal blob size D_{th} and chain Kuhn length b. Figure 1b illustrates different regimes of the dependence of the number of monomers per correlation length on monomer concentration together with the corresponding structures of chains of blobs and crossover concentrations. Thermal blobs start to overlap at monomer concentration $c = c_{th}$ where $g(c_{th}) = g_{th}$ or $\xi(c_{th}) = D_{th}$. Solving for concentration, we have

$$c_{th}l^3 = B_{th}^3 (B_{th}/B_g)^{1/(2\nu-1)}$$
(9)

As monomer concentration increases further, solution correlation length becomes comparable with the chain Kuhn length $\xi(c^{**}) = b$ and the number of monomers per correlation blob $g(c^{**}) = b/l$ at concentration $c = c^{**}$. Rewriting these conditions in terms of system parameters, we arrive at

$$c^{**}l^3 = B_{th}^4 \tag{10}$$

This is a crossover concentration to the concentrated solution regime. At monomer concentrations $c > c^{**}$, chains are rodlike on length scales smaller than the Kuhn length. For such chain conformations, the solution correlation length ξ is given by eq 6 with parameter B = 1 and exponent v = 1, $\xi = (cl)^{-0.5}$, and $g = (cl^3)^{-0.5}$ as shown in Figure 1b.

Thus, knowing crossover concentrations c^* , c_{th} , and c^{**} or parameters $B_{\rm g}$ and B_{th} , we can calculate the concentration dependences of the solution correlation length and the number of monomers per blob according to eqs 6 and 7. Below, we will show how these parameters can be obtained from analysis of solution viscosity.

As in the case of static chain properties, the scaling model of chain dynamics in semidilute solutions assumes that exponential screening of the hydrodynamic interactions between chains takes place at the characteristic length scale ξ_H proportional to the solution correlation length, $\xi_H \approx \xi$, with the proportionality coefficient on the order of unity.² In the interval of monomer concentrations $c < c^{**}$, chain dynamics is that of a chain of N/g correlation blobs with an effective friction coefficient ζ per blob. The friction coefficient is estimated by taking into account that on the length scales smaller than hydrodynamic correlation length ξ_{H} , there is a strong hydrodynamic coupling between the motion of chain sections with g monomers. This results in the effective friction coefficient $\zeta \approx \eta_s \xi_H$ in solutions with solvent viscosity η_s and the Zimm relaxation time^{4,12,14} of the correlation blob $\tau_{\xi} \approx$ $\eta_s \xi^3/k_B T$, where k_B is the Boltzmann constant and T is the absolute temperature.

At concentrations $c>c^{***}$, there are two different length scales—solution correlation length ξ , determining the length scale of the screening of hydrodynamic interactions, and Kuhn length, b, defining chain statistics. A chain can be effectively viewed as a chain of Kuhn segments each containing $g_b=b/l$ of the chemical monomers. The segment friction coefficient is calculated by summing up contributions from all correlation blobs within a Kuhn length. This results in the concentration-independent friction coefficient, $\zeta\approx\eta_s\xi b/gl\approx\eta_s b$ (neglecting logarithmic corrections), and the relaxation time of a Kuhn segment $\tau_b\approx\eta_s b^3/k_BT$.

In the framework of the scaling approach, the longest chain relaxation time in unentangled (Rouse) and entangled solution regimes can be written as follows

$$\tau = \tau_R(N)(1 + N/N_e) \tag{11}$$

where $\tau_R(N) = \tau_s N_s^2$ is the Rouse relaxation time of a chain of $N_s = N/g$ correlation blobs with characteristic relaxation time $\tau_s = \tau_\xi$ or $N_s = Nl/b$ Kuhn segments with $\tau_s = \tau_b$ for monomer concentrations $c < c^{***}$ and $c^{***} < c$, respectively.

The solution specific viscosity $\eta_{sp} = (\eta - \eta_s)/\eta_s$ is estimated from the product of the terminal or plateau shear modulus

$$G = k_{\rm B} Tc \begin{cases} N^{-1}, & \text{for } N < N_e \\ N_e^{-1}, & \text{for } N_e \le N \end{cases}$$
(12)

and the chain relaxation time (eq 11) as follows

$$\eta_{\rm sp} = \frac{G\tau}{\eta_{\rm s}} = N(1 + (N/N_{\rm e})^2) \begin{cases} g^{-1}, & \text{for } c \le c ** \\ cbl^2, & \text{for } c ** < c \end{cases}$$
(13)

It is important to make a couple of comments before proceeding further. (i) In eqs 11–13, we use an "=" sign, which means that we absorb all numerical coefficients into the definition of the B parameters determining the number of monomers per correlation blob and the number of monomers between entanglements as discussed below. (ii) In deriving expressions for chain relaxation time and solution viscosity, we use the original de Gennes approach resulting in $\eta_{\rm sp} \sim N^3$ in the entangled solution regime. A stronger N-dependence $\eta \sim N^{3.4}$ is observed in well-entangled polymer melts, $N > 10N_e$, and is proven to be due to tube length fluctuations.

The number of monomers between entanglements N_e is calculated by using the Kavassalis–Noolandi conjecture $^{26-28}$ in good solvents for the polymer or the Rubinstein–Colby conjecture 11,13,29 in θ solvents and marginally good solvents. This analysis is overviewed in the Supporting Information, and here, we only present the final results. In a good solvent with $c_{th}b^3 \geq 1$ (which is equivalent to the condition $B_{\rm g} \leq B_{th}^{4}$ $^{6\nu}$), applying the Kavassalis–Noolandi conjecture, we obtain

$$N_{e} = P_{e}^{2} \begin{cases} g, & \text{for } c \leq c *** \\ c^{-2} (lb)^{-3}, & \text{for } c ** < c \end{cases}$$
 (14)

where P_e is the packing number (the number of entanglement strands per tube diameter). In a θ or marginally good solvent with $c_{th}b^3 < 1$ ($B_{\rm g} > B_{th}^{4-6\nu}$), calculations in the framework of the Rubinstein–Colby approach lead to

$$N_e = P_e^2 \begin{cases} (c_{th}b^3)^{2/3}g, & \text{for } c \le c_{th} \\ B_{th}^2(cl^3)^{-4/3}, & \text{for } c_{th} < c \le b^{-3} \end{cases}$$
 (15)

Note that in the concentration interval $cb^3 > 1$, the number of monomers between entanglements N_e is given by eq 14.

Before using eq 13 for analysis of experimental data, we have to account for system polydispersity. This is done by averaging eq 13 over a distribution of chain degrees of polymerization. The details of these calculations are given in the Supporting Information. For a Schulz–Zimm distribution 30,31 of chain degrees of polymerization, this analysis results in

$$\eta_{\rm sp} = N_{\rm w} \left(1 + \frac{(k+3)(k+2)}{(k+1)^2} \left(\frac{N_{\rm w}}{N_{\rm e}} \right)^2 \right) \left\{ g^{-1}, \text{ for } c \le c ** \\ cbl^2, \text{ for } c ** < c \end{cases}$$
(16)

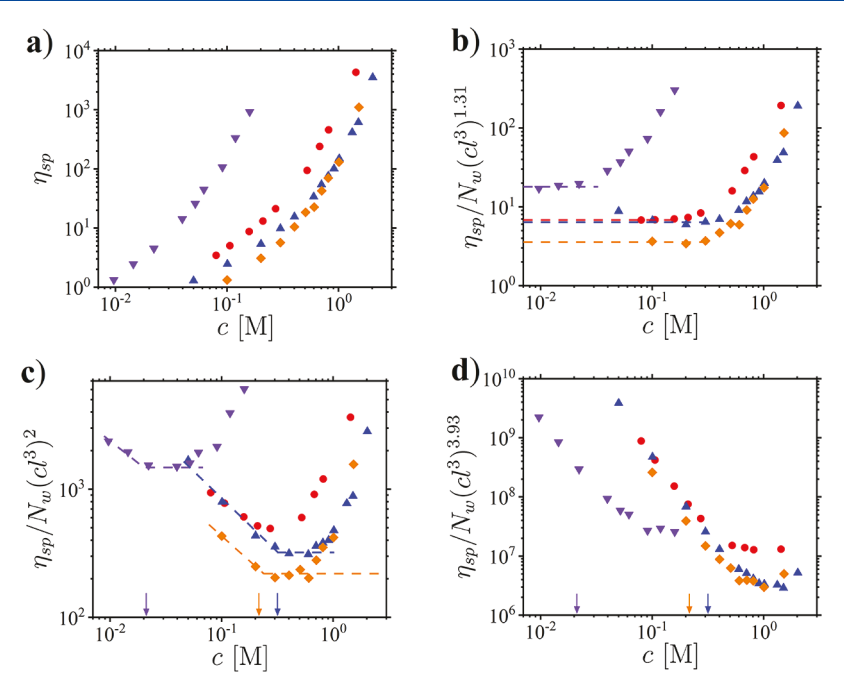


Figure 2. Dependence of specific viscosity (a) and normalized specific viscosity (b) $\eta_{\rm sp}/N_{\rm w}(cl^3)^{1.31}$, (c) $\eta_{\rm sp}/N_{\rm w}(cl^3)^2$, and (d) $\eta_{\rm sp}/N_{\rm w}(cl^3)^{3.93}$ on chemical monomer concentration c expressed in moles of monomers per liter [M] for solutions of poly(styrene) with $N_{\rm w}=5769$ in tetrahydrofuran (red circles) at 303 K, poly(methyl methacrylate) with $N_{\rm w}=3061$ in ionic liquids $[C_4({\rm mim})][{\rm TFSI}]$ (blue triangles) and $[C_8({\rm mim})_2][{\rm TFSI}]_2$ (orange rhombs) at 298 K, and NaCMC with $N_{\rm w}=889$ in 0.1 M NaCl aqueous solutions (violet inverted triangles) at 298 K. Values of the system-specific monomer projection lengths are given in Table 1. Lines and arrows of different colors in panels b—d show crossover concentrations and plateau values used for calculations of the B parameters listed in Table 1.

where N_w is the weight average degree of polymerization, and parameter $k \equiv 1/(\mathfrak{D}-1)$ depends on the system dispersity index $\mathfrak{D} \equiv N_w/N_n$.

ANALYSIS OF EXPERIMENTAL DATA

Our approach for obtaining the B parameters is based on the observation that in the Rouse regime of unentangled chains, $N_w < N_e$, specific viscosity is inversely proportional to the number of monomers in the correlation blob

$$\eta_{\rm sp} = N_{\rm w}/g, \text{ for } N_{\rm w} < N_e \tag{17}$$

At chain overlap concentration $c = c^*$, the number of monomers per correlation blob $g = N_w$, and specific viscosity $\eta_{\rm sp}$ = 1. These conditions define a reference point for calculations of the B parameters and crossover concentrations c_{th} and c^{**} . Taking into account the concentration dependence of g given by eq 7 and shown in Figure 1b, we can normalize specific viscosity $\eta_{\rm sp}$ by a factor $N_{\rm w}$ $(cl^3)^{1/(3\nu-1)}$ with the scaling exponent v determined by the blob type to eliminate the concentration dependence in the corresponding solution regime. This data representation allows us to obtain values of the B parameters from the resulting plateau values and crossover concentrations c_{th} and c^{**} from the locations of the plateaus or from the B parameters (see eqs 9 and 10). For example, at monomer concentrations $c^* < c < c_{th}$ on length scales on the order of solution correlation length, chain statistics is that of a self-avoiding walk with exponent v = 0.588and $g \sim (cl^3)^{-1.31}$ as shown in Figure 1b, resulting in a concentration-dependent part of the normalization factor $(cl^3)^{1.31}$, while for the concentration interval $c_{th} \le c \le c^{**}$, it is a random walk with $\nu = 0.5$ and $g \sim (cl^3)^{-2}$ for which the specific viscosity normalization factor is $(cl^3)^2$.

The approach outlined above is applied to poly(ethylene oxide) in water (PEO), 32 poly(styrene) in tetrahydrofuran (PS-THF) 33 and toluene (PS-Toluene), 34,35 poly(methyl methacrylate) in ionic liquids [C₄(mim)][TFSI] (PMMA-I) and [C₈(mim)₂][TFSI]₂ (PMMA-II), 36 and sodium carboxymethylcellulose (NaCMC) in 0.1 M NaCl aqueous solution. 37 At such high salt concentrations, the properties of polyelectrolyte solutions are similar to solutions of neutral polymers in a good solvent. 10 The complete data analysis for each polymer/solvent pair is given in the Supporting Information.

The main steps of the approach are illustrated in Figure 2 for the selected data sets of poly(styrene) in tetrahydrofuran with $N_{\rm w}=5769$, poly(methyl methacrylate) in ionic liquids, and sodium carboxymethylcellulose in water, of which the concentration dependences of the specific viscosity are shown in Figure 2a. In Figure 2b,c, we demonstrate how different crossover concentrations and values of the B parameters are determined from the replotted specific viscosity data. Figure 2b presents normalized specific viscosity $\eta_{\rm sp}/N_{\rm w}$ (cl³)^{1.31} as a function of monomer concentration. The parameters $B_{\rm g}$ are obtained from the plateau values C_p , indicated by the dashed lines, as

$$B_{\rm g} = C_p^{-\nu + 1/3} = C_p^{-0.255} \tag{18}$$

with v = 0.588, the exact exponent for a self-avoiding walk.

Figure 2c shows normalized specific viscosity data $\eta_{\rm sp}/N_{\rm w}$ $(cl^3)^2$ suitable for extracting crossover concentration c_{th} , where locations are pointed out by colored arrows. The values of the parameter B_{th} are determined from the thermal blob overlap concentration c_{th} and parameter $B_{\rm g}$

$$B_{th} = (c_{th}l^3)^{(2\nu-1)/(6\nu-2)} B_g^{1/(6\nu-2)}$$
(19)

Table 1. Summary of Parameters for Studied Systems^a

system	$N_{\scriptscriptstyle w}$	$B_{ m g}$	B_{th}	c_{th} [M]	c** [M]	b [nm]	g_{th}	$c_{th}b^3$	P_e
PEO	9091-90,909	1.12	0.62	0.35	6.30	0.88	846	0.15	$7.2^{(1)}$
PS-THF	3750-75,000	0.61							$6.7^{(2)}$
PS-Toluene	2558-227,000	0.74	0.42	0.33	3.27	1.41	536	0.56	4.4 ⁽¹⁾
PMMA-I	3061	0.62	0.38	0.32	2.05	1.78	296	1.07	16.0 ⁽³⁾
PMMA-II	3061	0.72	0.41	0.25	2.70	1.55	712	0.56	10.3 ⁽³⁾
NaCMC	889	0.48	0.30	0.021	0.094	5.85	229	2.5	$9.5^{(1)}$

"PEO — aqueous solutions of poly(ethylene oxide) with weight average molecular weights $M_{\rm w}=4\times10^5$, 1×10^6 , and 4×10^6 g/mol, monomer molecular weight $M_0=44$ g/mol, and monomer projection length l=0.338 nm calculated using ChemDraw. PS-THF — tetrahydrofuran solutions of poly(styrene) with $M_{\rm w}=7.8\times10^6$, 1.8×10^6 , 6.0×10^5 , and 3.9×10^5 g/mol, $M_0=104$ g/mol, l=0.255 nm, and D=1.1. PS-Toluene — solutions of poly(styrene) in toluene with $M_{\rm w}$ between 2.66×10^5 and 2.36×10^7 g/mol, $M_0=104$ g/mol, and l=0.255. PMMA-I and PMMA-II are solutions of poly(methyl methacrylate) in ionic liquids $[C_4(\text{mim})][\text{TFSI}]$ and $[C_8(\text{mim})_2][\text{TFSI}]_2$, respectively, and with $M_{\rm w}=3.061\times10^5$ g/mol, $M_0=100$ g/mol, l=0.255 nm, and D=1.74. NaCMC — aqueous solutions of sodium carboxymethylcellulose in 0.1 M NaCl with $M_{\rm w}=2.4\times10^5$ g/mol, $M_0=270$ g/mol, and l=0.515 nm. Kuhn length $b=lB_{th}^{-2}$ and the number of monomers in a thermal blob $g_{th}=(B_g/B_{th})^{2/(2\nu-1)}$ with exponent $\nu=0.588$. (1) Reported values correspond to the apparent packing number. (2,3) Values of the packing number are calculated by using eq 21 with k=1/(D-1) values obtained from D=1.1 and D=1.74 reported in refs 33 and 34 for PS-THF and PMMA systems, respectively.

Note that values of the B_{th} parameter can also be calculated from the intermediate plateau values C_p as $B_{th} = C_p^{-1/6}$. Values of B_{th} obtained by this procedure are consistent with those calculated using crossover concentration locations and B_g . Substituting B_{th} into eq 10, we determine the crossover concentration to the concentrated solution regime, c^{**} . Results of this analysis are summarized in Table 1.

Finally, the plot $\eta_{\rm sp}/N_{\rm w}$ $(cl^3)^{3.93}$, where exponent 3.93 = 3/ $(3\nu-1)$ for $\nu=0.588$ corresponds to $\eta_{\rm sp}\sim g^{-3}$, as a function of monomer concentration (see Figure 2d) serves as a self-consistency check that the crossover to the entangled solution regime does not influence the location of the crossover concentration into the thermal blob overlap regime. In particular, this analysis points out that for the PS-THF system, the observed minimum in Figure 2c is due to a crossover to the entangled solution regime as discussed in the Supporting Information.

Analysis of the data in Table 1 for the Kuhn length indicates that packing of the solvent around the polymer backbone could increase chain stiffness even for identical polymers as observed for PMMA in ionic liquids. This is unique information, which is difficult to obtain by other techniques. We can describe the solvent quality by the number of monomers per thermal blob, g_{th} . This representation is more convenient than the value of the second virial coefficient since it immediately indicates how long a chain should be to experience binary polymer—polymer interactions and swell. Specifically, the values listed in Table 1 point out that the NaCMC system is in the best solvent, while PEO is in the worst one among the studied solutions. Information summarized in Table 1 is used to calculate the concentration dependence of the solution correlation length in the different solution regimes as shown in Figure 3.

Due to the different concentration dependences of the number of monomers per correlation blob (see eq 7) and the number of monomers between entanglements N_{ϵ} (eqs 14 and 15), we need to rescale solution viscosity to plot the data in terms of the number of blobs per chain. For systems with $c_{th}b^3 \ge 1$ ($B_{\rm g} \le B_{th}^{4-6\nu}$), we have the following universal function for solution-specific viscosity

$$\lambda \eta_{\rm sp} = (N_{\rm w}/\tilde{\rm g})(1 + \tilde{P}_e^{-4}(N_{\rm w}/\tilde{\rm g})^2)$$
 (20)

where the multiplication factor $\lambda = 1$ for $c \le c^{**}$, and $\lambda = c/c^{**}$ for $c^{**} < c$. The number of monomers per normalization blob $\tilde{g} = g$ (eq 7) for $c \le c^{**}$, and $\tilde{g} = B_{th}^{-2}(c^{**}/c)^2$ for $c^{**} < c$. We

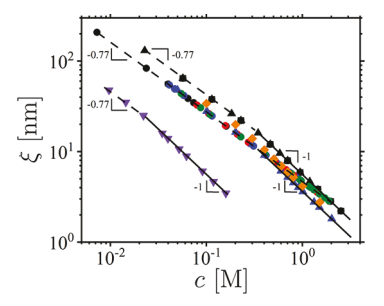


Figure 3. Dependence of the solution correlation length ξ on chemical monomer concentration c expressed in moles of monomers per liter [M] for aqueous solutions of poly(ethylene oxide) (PEO) with $N_w = 9091$ (black squares), 22,727 (black circles), and 90,909 (black triangles); tetrahydrofuran solutions of poly(styrene) with $N_w = 3750$ (green circles), 5769 (red circles), 17,308 (blue circles), and 75,000 (black circles); poly(methyl methacrylate) in ionic liquids [C₄(mim)][TFSI] (blue triangles) (PMMA-I) and [C₈(mim)₂]-[TFSI]₂ (PMMA-II) (orange rhombs); and NaCMC in 0.1 M NaCl solution (violet inverted triangles). The solution correlation length is calculated using eq 6 with monomer projection lengths l and values of the B parameters from Table 1.

can hide system polydispersity information by introducing the apparent packing number

$$\tilde{P}_{e} = ((k+1)^{2}/(k+3)(k+2))^{1/4}P_{e}$$
(21)

This value is reported below if no information about system polydispersity is given.

In the case of θ or marginally good solvents ($c_{th}b^3 < 1$ or $B_{\rm g} > B_{th}^{4-6\nu}$), to account for different concentration dependences of the number of monomers between entanglements N_e (see eqs 14 and 15) and the number of monomers per correlation blob (eq 7), we have to perform the following transformations: (i) introduce the normalized packing number

$$P_{e,RC} = P_e (c_{th} b^3)^{1/3} (22)$$

to reduce eq 15 to a form similar to eq 14 in the concentration interval $c \le c_{th}$ and (ii) define the number of monomers in a normalization blob $\tilde{g} = \lambda_g g$ with a rescaling factor

Macromolecules Article pubs.acs.org/Macromolecules

$$\lambda_{g} = \begin{cases} 1, & \text{for } c \leq c_{th} \\ (c/c_{th})^{2/3}, & \text{for } c_{th} < c \leq b^{-3} \\ (c_{th}b^{3})^{-2/3}, & \text{for } b^{-3} < c \end{cases}$$
(23)

This rescaling allows for a representation of the solutionspecific viscosity data in a universal functional form similar to eq 20 with P_e in the expression for the apparent packing number \tilde{P}_e (eq 21) substituted by $P_{e,RC}$, the number of monomers in the normalization blob $\tilde{g} = \lambda_g g$, and multiplication factor λ defined as $\lambda = \lambda_g^{-1}$ for $c \le c^{***}$ and $\lambda = (c/c^{**}) \lambda_g^{-1}$ for $c^{**} < c$.

By applying the criterion $c_{th}b^3$ to the studied systems, we find that for aqueous solutions of PEO, PS-Toluene, and PMMA-II, it is smaller than unity (see Table 1), and it is bigger than unity for PMMA-I and NaCMC. It cannot be determined for PS-THF systems since we are unable to locate thermal blob overlap concentration c_{th} . This classification allows us to determine how to represent viscosity data in a universal form and to obtain the packing number. Figure 4 shows the universal specific viscosity plots using the rescaling procedure

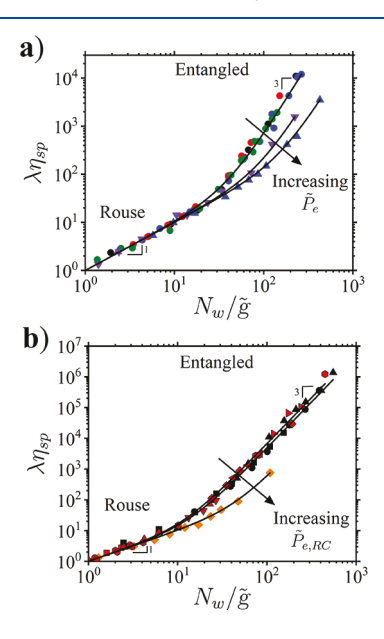


Figure 4. (a) Dependence of the normalized specific viscosity $\lambda \eta_{sp}$ = $\lambda(\eta - \eta_s)/\eta_s$ on the number of blobs per chain N_w/\tilde{g} for tetrahydrofuran solutions of poly(styrene) with $N_w = 3750$ (green circles), 5769 (red circles), 17,308 (blue circles), and 75,000 (black circles); poly(methyl methacrylate) in ionic liquid $[C_4(mim)][TFSI]$ (PMMA-I) (blue triangles); and NaCMC in 0.1 M NaCl solution (violet inverted triangles). Multiplication factor $\lambda = 1$ for $c \le c^{**}$ and $\lambda = c/c^{**}$ for $c^{**} < c$. The number of monomers per blob $\tilde{g} = g$ is given by eq 7 for $c \le c^{**}$ and $g = B_{th}^{-2}(c^{**}/c)^2$ for $c > c^{**}$. Solid lines are the best fits to eq 20 with \tilde{P}_{ϵ} as a fitting parameter. (b) Dependence of the normalized specific viscosity $\lambda \eta_{\rm sp}$ on the number of blobs per chain N_w/\tilde{g} for aqueous solutions of poly(ethylene oxide) (PEO) with N_w = 9091 (black squares), 22,727 (black circles), and 90,909 (black triangles); poly(methyl methacrylate) in ionic liquid [C₈(mim)₂][TFSI]₂ (PMMA-II) (orange rhombs); and toluene solutions of poly(styrene) with N_w between 2558 and 227,000 (red symbols). The number of monomers per blob $\tilde{g}=\lambda_g g$ where λ_g is calculated according to eq 23, g is given by eq 7 for $c \le c^{**}$, and $g = B_{th}^{-2}(c^{**}/c)^2$ for $c > c^{**}$. Multiplication factor $\lambda = \lambda_g^{-1}$ for $c \le c^{**}$ and $\lambda = (c/c^{**})$ λ_g^{-1} for $c^{**} < c$. Solid lines are the best fits to eq 20 with $\tilde{P}_{e, RC}$ as a fitting parameter.

described above. It follows from this figure that all data sets demonstrate qualitatively similar behavior.

For a small number of blobs per chain, system dynamics is described by unentangled (Rouse) chain dynamics with specific viscosity increasing linearly with the number of blobs per chain. As the number of blobs per chain increases further, we see a stronger dependence of the solution viscosity on the number of blobs. In particular, at $N_w/\tilde{g} > 10 \div 30$, there is a crossover to an entangled solution regime with $\lambda \eta_{\rm sp} \sim (N_{\scriptscriptstyle W}/\tilde{\rm g})^3$. The values of the packing numbers P_{e} , obtained by fitting viscosity data to eq 20, are between 4.4 and 16.0. These values appear to be small in comparison with those known for polymer melts $(P_e = 20-24)^{1.14}$ Note that for systems with unreported dispersity, we report the apparent packing number,

All viscosity data sets shown in Figure 4 can be collapsed together by plotting reduced viscosity as a function of the number of entanglements per chain

$$\lambda \eta_{\rm sp} / \tilde{P}_e^2 = (N_{\rm w} / \tilde{N}_e) (1 + (N_{\rm w} / \tilde{N}_e)^2) \tag{24}$$

where $\tilde{N}_e = \tilde{P}_e^2 \tilde{g}$ is an effective number of monomers between entanglements. This data representation is shown in Figure 5

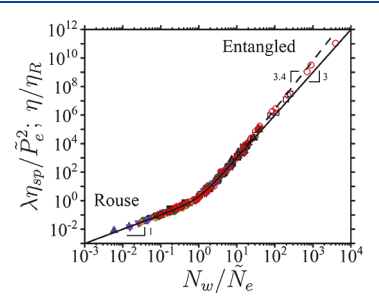


Figure 5. Dependence of the normalized specific viscosity $\lambda \eta_{sp}/\tilde{P}_e^2$ on the number of entanglements per chains $\bar{N_w}/\tilde{N_e}$ for solutions of PEO in water at 293 K, PS in THF at 303 K, PS in toluene at 298 K, PMMA in ionic liquids at 298 K, and NaCMC in 0.1 M NaCl aqueous solutions at 298 K. Notations are the same as in Figure 4. The number of monomers between entanglements is calculated according to $\tilde{N}_{\varepsilon} = \tilde{P}_{\varepsilon}^2 \tilde{\mathbf{g}}$. Viscosity data for melts of polyisobutylene at 490 K (open black squares) and polybutadiene at 298 K (open red circles) are represented as normalized viscosity η/η_R vs N_w/N_e .

together with data for melts of polyisobutylene 38-40 and polybutadiene. 41 To superimpose solution and melt data, we normalized melt viscosity η by $\eta_R = \eta(\tilde{N}_e)/2$ half of the melt viscosity at $N_w = N_e$ corresponding to the crossover from the Rouse to the entangled melt regime (see the Supporting Information). It follows from this figure that melt and solution data overlap for $N_w/\tilde{N}_e < 10$, while for $N_w/\tilde{N}_e > 10$, the melt viscosity data demonstrate clear departure from $\eta \sim (N_w/\tilde{N}_e)^3$ scaling dependence, approaching a stronger $\eta \sim (N_w/\tilde{N}_e)^{3.4}$ increase with the number of entanglements per chain. The difference in crossovers between melts and solutions could be due to a difference in the "softness" of the tube length fluctuation mode in solutions and melts. Unfortunately, with the available data, it is impossible to say with confidence where the PEO data will show a dependence of viscosity similar to melts, $\eta \sim (N_w/\tilde{N}_e)^{3.4}$. Addressing this issue requires additional studies of solution rheology on samples with longer chains.

CONCLUSIONS

We have developed an approach for calculations of the B parameters and crossover concentrations into different solution regimes. This approach takes advantage of the linear dependence of the specific viscosity on the number of correlation blobs per chain in the Rouse regime (eq 17) such that the values of the B parameters and crossover concentrations are derived from plots of the concentration dependence of the normalized specific viscosity $\eta_{\rm sp}/N_{\scriptscriptstyle W}~(cl^3)^{1.31}$ and $\eta_{\rm sp}/N_{\rm w}$ (cl^3)² (see Figure 2b,c). The B parameters are then used to calculate solution correlation length (Figure 3) and to represent specific viscosity in terms of the number of blobs per chain, N_w/\tilde{g} (Figure 4). This universal data representation provides a means to extract the packing number, P_e . After this is done, we have a set of parameters $\{B_g, B_{th}, P_e\}$ uniquely describing a polymer/solvent pair (a system "fingerprint"). Using this information, we evaluated the Kuhn length and the number of monomers per thermal blob, describing the strength of interactions for a given polymer/solvent pair as shown in Table 1. Furthermore, by obtaining the concentration dependence of the number of monomers between entanglements, we collapsed viscosity data of polymer solutions and melts (see Figure 5), highlighting the universality of their behavior in regimes with Rouse and entangled chain dynamics.

Note that by assembling the set of parameters $\{B_{\rm g}, B_{\rm th}, P_e\}$ for different polymer/solvent pairs, one creates a library that can be used for analysis and prediction of polymer solution properties. In particular, it could be used to quantitatively predict concentration dependence of chain size (eq 1), correlation length (eq 6), relaxation time (eq 11), and solution viscosity (eq 16) for polymers with a known molecular weight distribution. We can also take advantage of the linear dependence of the solution viscosity on the weight average degree of polymerization N_w in the Rouse regime to obtain/verify molecular weight.

Our approach breaks down at high monomer concentrations, $cl^3 \geq 1$, at which solvent distribution around the polymers is influenced by the presence of neighboring chains. At such high monomer concentrations, one also has to consider the renormalization of the monomeric friction coefficient to account for additional concentration dependences of system viscosity and relaxation time. This was shown to be important to correctly describe chain dynamics in concentrated solutions of charged 42 and neutral polymers and melts. 40

A two-parameter scaling approach to quantitatively describe static and dynamic properties of entangled semidilute polymer solutions was developed by Raspaud el al.⁴³ and applied by Musti et al. to DNA solutions.⁴⁴ Their method is based on a combination of osmometry, scattering, and rheological techniques and assumes a priori that chain conformations on length scales smaller than the solution correlation length remain unchanged in the semidilute solution regime. The obvious advantages of our approach are that it only requires knowledge of the concentration dependence of solution viscosity, is free of any a priori assumptions about chain statistics on length scales of the solution correlation length, and explicitly includes polymer dispersity.

At the end, we would like to comment that the developed approach can be extended to polyelectrolyte solutions by accounting for electrostatic blobs and their overlap concentration ^{10,45–48} as described in ref 49. It could also be applied to

the characterization of graft polymers. 50,51 The obtained set of parameters $\{B_g, B_{th}, P_e\}$ could be used for quantitative analysis of gel swelling data 17,19 and thickness of polymer chains in brush layers. 21,22,24 The developed approach can be adapted to obtain B parameters from osmotic pressure data in different solution regimes. We hope that this work will inspire such investigations.

ASSOCIATED CONTENT

Supporting Information

The Supporting Information is available free of charge at https://pubs.acs.org/doi/10.1021/acs.macromol.0c02810.

List of notations, calculations of N_e , data analysis, and effects of chain polydispersity (PDF)

AUTHOR INFORMATION

Corresponding Author

Andrey V. Dobrynin — Department of Chemistry, University of North Carolina, Chapel Hill, North Carolina 27599-3290, United States; orcid.org/0000-0002-6484-7409; Email: avd@email.unc.edu

Authors

Michael Jacobs — Department of Chemistry, University of North Carolina, Chapel Hill, North Carolina 27599-3290, United States; © orcid.org/0000-0002-7255-3451

Ryan Sayko — Department of Chemistry, University of North Carolina, Chapel Hill, North Carolina 27599-3290, United States; oocid.org/0000-0002-5986-4829

Complete contact information is available at: https://pubs.acs.org/10.1021/acs.macromol.0c02810

Notes

The authors declare no competing financial interest.

ACKNOWLEDGMENTS

This work was supported by the National Science Foundation under the grants DMREF- 2049518 and 1921923. A.V.D. is grateful to Ralph Colby for discussions on viscosity of polymer melts.

REFERENCES

- (1) de Gennes, P. G., Scaling Concepts in Polymer Physics; Cornell University Press: Ithaca, NY, 1979.
- (2) de Gennes, P. G. Dynamics of Entangled Polymer Solutions. I. The Rouse Model. *Macromolecules* **1976**, *9*, 587–593.
- (3) de Gennes, P. G. Dynamics of Entangled Polymer Solutions. II. Inclusion of Hydrodynamic Interactions. *Macromolecules* **1976**, *9*, 594–598.
- (4) Doi, M.; Edwards, S. F., The theory of polymer dynamics. Oxford University Press: New York, 1986.
- (5) Cates, M. E. Statics and Dynamics of Polymeric Fractals. *Phys. Rev. Lett.* **1984**, *53*, 926–929.
- (6) Adam, M.; Delsanti, M. Viscosity and longest relaxation time of semi-dilute polymer solutions. I. Good solvent. *J. Phys. (France)* **1983**, 44, 1185–1193.
- (7) Adam, M.; Delsanti, M. Dynamical Behavior of Semidilute Polymer Solutions in a Θ Solvent: Quasi-Elastic Light Scattering Experiments. *Macromolecules* **1985**, *18*, 1760–1770.
- (8) de Gennes, P. G. Towards a scaling theory of drag reduction. *Physica A* **1986**, *140*, 9–25.
- (9) Brochard, F.; de Gennes, P. G. Dynamics of confined polymer chains. J. Chem. Phys. 1977, 67, 52-56.

- (10) Dobrynin, A. V.; Rubinstein, M. Theory of polyelectrolytes in solutions and at surfaces. *Prog. Polym. Sci.* **2005**, *30*, 1049–1118.
- (11) Colby, R. H.; Rubinstein, M. Two-Parameter Scaling for Polymers in Θ Solvents. *Macromolecules* **1990**, 23, 2753–2757.
- (12) Grosberg, A. Y.; Khokhlov, A. R., Statistical Physics of Macromolecules. AIP Press: 1994.
- (13) Heo, Y.; Larson, R. G. Universal Scaling of Linear and Nonlinear Rheological Properties of Semidilute and Concentrated Polymer Solutions. *Macromolecules* **2008**, *41*, 8903–8915.
- (14) Rubinstein, M.; Colby, R. H., Polymer Physics; Oxford University Press: New York, NY, 2003.
- (15) Pincus, P. Excluded Volume Effects and Stretched Polymer Chains. *Macromolecules* **1976**, *9*, 386–388.
- (16) Pincus, P. Dynamics of Stretched Polymer Chains. *Macromolecules* 1977, 10, 210-213.
- (17) Candau, S.; Bastide, J.; Delsanti, M. Structural, Elastic, and Dynamic Properties of Swollen Polymer Networks. *Adv. Polym. Sci.* **1982**, 27–71.
- (18) Harden, J. L.; Cates, M. E. Deformation of grafted polymer layers in strong shear flows. *Phys. Rev. E* **1996**, *53*, 3782–3787.
- (19) Canal, T.; Peppas, N. A. Correlation between mesh size and equilibrium degree of swelling of polymeric networks. *J. Biomed. Mater. Res.* **1989**, 23, 1183–1193.
- (20) Milner, S. T.; Witten, T. A.; Cates, M. E. Theory of the Grafted Polymer Brush. *Macromolecules* **1988**, *21*, 2610–2619.
- (21) Milner, S. T. P. B. Science 1991, 251, 905.
- (22) Binder, K. Scaling concenpts for polymer brushes and their test with computer simulations. *Eur. Phys. J. E* **2002**, *9*, 293–298.
- (23) Chen, W.-L.; Cordero, R.; Tran, H.; Ober, C. K. 50th Anniversary Perspective: Polymer brushes: Novel surfaces for future materials. *Macromolecules* **2017**, *50*, 4089–4113.
- (24) Grest, G. S. Normal and shear forces between polymer brushes. *Adv. Polym. Sci.* **1999**, *138*, 149–183.
- (25) Ahlrichs, P.; Everaers, R.; Dunweg, B. Screening of hydrodynamic interactions in semidilute polymer solutions: a computer simulation study. *Phys. Rev. E* **2001**, *64*, No. 040501.
- (26) Kavassalis, T. A.; Noolandi, J. New view of entanglements in dense polymer systems. *Phys. Rev. Lett.* **1987**, *59*, 2674–2677.
- (27) Kavassalis, T. A.; Noolandi, J. A new theory of entanglements and dynamics in dense polymer systems. *Macromolecules* **1988**, *21*, 2869–2879.
- (28) Kavassalis, T. A.; Noolandi, J. Entanglement scaling in polymer melts and solutions. *Macromolecules* **1989**, 22, 2709–2720.
- (29) Milner, S. T. Predicting tube diameter in melts and solutions. *Macromolecules* **2005**, *38*, 4929–4939.
- (30) Schulz, G. V. The kinetics of chain polymerisation V. The influence of various types of reactions on the poly-molecularity. *Z. Phys. Chem.* **1939**, *B43*, 25–46.
- (31) Zimm, B. H. Apparatus and methods for measurement and interpretation of the angular variation of light scattering: Preliminary results on polystyrene solutions. *J. Chem. Phys.* **1948**, *16*, 1099–1117.
- (32) Ebagninin, K. W.; Benchabane, A.; Bekkour, K. Rheological characterization of poly(ethylene oxide) solutions of different molecular weights. *J. Colloid Interface Sci.* **2009**, 336, 360–367.
- (33) Jamieson, A. M.; Telford, D. Newtonian Viscosity of Semidilute Solutions of Polystyrene in Tetrahydrofuran. *Macromolecules* **1982**, *15*, 1329–1332.
- (34) Kulicke, W.-M.; Kniewske, R. The shear viscosity dependence on concentration, molecular weight, and shear rate of polystyrene solutions. *Rheol. Acta* **1984**, 23, 75–83.
- (35) Zakin, J. L.; Wu, R.; Luh, H.; Mayhan, K. G. Generalized correlations for molecular weight and concentration dependence of zero-shear viscosity of high polymer solutions. *J. Polym. Sci. B: Polym. Phys* **1979**, *14*, 299–308.
- (36) He, X.; Kong, M.; Niu, Y.; Li, G. Entanglement and Relaxation of Poly(methyl methacrylate) Chains in Imidazolium-Based Ionic Liquids with Different Cationic Structures. *Macromolecules* **2020**, *53*, 7865–7875.

- (37) Lopez, C. G. Entanglement of semiflexible polyelectrolytes: Crossover concentrations and entanglement density of sodium carboxymethyl cellulose. *J. Rheol.* **2020**, *64*, 191–204.
- (38) Fox, T. G.; Flory, P. J. Viscosity-Molecular Weight and Viscosity-Temperature Relationships for Polystyrene and Polyisobutylene. *JACS* **1948**, *70*, 2384–2395.
- (39) Fox, T. G.; Flory, P. J. Further Studies on the Melt Viscosity of Polyisobutylene. *J. Phys. Chem.* **1951**, *55*, 221–234.
- (40) Berry, G. C.; Fox, T. G. The Viscosity of Polymers and Their Concentrated Solutions. *Adv. Polym. Sci.* 1968, 5, 261–357.
- (41) Colby, R. H.; Fetters, L. J.; Graessley, W. W. Melt Viscosity-Molecular Weight Relationship for Linear Polymers. *Macromolecules* 1987, 20, 2226–2237.
- (42) Liao, Q.; Carrillo, J.-M. Y.; Dobrynin, A. V.; Rubinstein, M. Rouse Dynamics of Polyelectrolyte Solutions: Molecular Dynamics Study. *Macromolecules* **2007**, *40*, 7671–7679.
- (43) Raspaud, E.; Lairez, D.; Adam, M. On the Number of Blobs per Entanglement in Semidilute and Good Solvent Solution: Melt Influence. *Macromolecules* **1995**, 28, 927–933.
- (44) Musti, R.; Sikorav, J.-L.; Lairez, D.; Jannink, G.; Adam, M. Viscoelastic properties of entangled DNA solutions. *C. R. Acad. Sci. Paris* **1995**, 320, 599–605.
- (45) de Gennes, P. G.; Pincus, P.; Brochard, F.; Velasco, R. M. Remarks on polyelectrolyte conformation. *J. de Phys.* **1976**, *37*, 1461–1476
- (46) Dobrynin, A. V.; Colby, R. H.; Rubinstein, M. Scaling theory of polyelectrolyte solutions. *Macromolecules* **1995**, 28, 1859–1871.
- (47) Muthukumar, M. 50th anniversary perspective: A perspective on polyelectrolyte solutions. *Macromolecules* **2017**, *50*, 9528–9560.
- (48) Dobrynin, A. V. Polyelectrolytes: On the door steps of the second century. *Polymer* **2020**, 202, 122714–1-13.
- (49) Dobrynin, A. V.; Jacobs, M. When do polyelectrolytes entangle? *Macromolecules* **2021** DOI: 10.1021/acs.macromol.0c02450.
- (50) Sheiko, S. S.; Sumerlin, B. S.; Matyjaszewski, K. Cylindrical Molecular Brushes: Synthesis, Characterization, and Properties. *Prog. Polym. Sci.* **2008**, *33*, 759–785.
- (51) Xie, G.; Martinez, M. R.; Olszewski, M.; Sheiko, S. S.; Matyjaszewski, K. Molecular bottlebrushes as novel materials. *Biomacromolecules* **2019**, 20, 27–54.